Journal of Chemistry and Environment

Research Article

Synthesis and Photoluminescent Study of Dy Doped Ca$_3$Gd$_2$(BO$_3$)$_4$ Phosphors

Majid Ali[1†], Hammad Haider[1†], Fawad Ullah[*1] Muhammad Bilal[2*], Shahzad Nawaz Malik[3]

[1]Department of Physics, Kohat University of Science and Technology, Khyber Pakhtunkhwa, Pakistan.
[2]School of Chemistry, and Xi'an Key Laboratory of Sustainable Energy Materials Chemistry, Xi'an Jiao Tong University, Xi'an 710049, P. R. China
[3]Department of Physics, COMSATS University Islamabad, Islamabad, 45550, Pakistan.
[†]These authors contributed equally.

*Correspondence: (Fawad Ullah)
fawadullah@gmail.com
(Muhammad Bilal)
bilalkhankarimo44@gmail.com

Abstract
The synthesis and photoluminescence study of Dysprosium (Dy) doped Calcium Gadolinium Borate Ca$_3$Gd$_2$(BO$_3$)$_4$:Dy^{3+} are presented in this research. The aim of this study was to investigate the optical properties and potential applications of Dy-doped Calcium Gadolinium Borate as a luminescent material. The samples with Dy^{+3} doping have been synthesized by the solid state reaction method at varying concentration of Dy^{+3} ions. The phase purity of the synthesized samples was confirmed from the X-ray diffraction where single phase orthorhombic structure was obtained. The UV excitation photoluminescence spectra of synthesized samples and emission peaks referring to the energy transition of Dy^{+3} ions are identified. Here, different emission intensities and the shift in the peaks position with reference to change in the Dy^{+3} concentration were analyzed, and the maximum luminescence intensity was observed at the best dopant concentration. This is made evident from this concentration-dependent behavior which suggests that energy transfer from the host lattice to Dy^{+3} ions is highly efficient. Therefore, the present work is a successful path towards Dy-doped Calcium Gadolinium Borate as a luminescent material. Due to its property this material seems to have good application potential in solid-state lighting, display and opto-sensing.

Keywords: Calcium Gadolinium Borate, photoluminescence, luminescent materials, solid-state reaction.

1. Introduction

Naturally, the vast majority of energy exists at the very high range. While the majority of applications just need little energy. Phosphors are light-emitting substances made of host matrix with a little quantity of rare-earth or transition metal ions serving as activators [1]. These materials have the ability to undergo electronic transitions that shift light from a higher to a lower frequency [2]. With the emergence of inorganic phosphor, a new achievement in the study of luminescence has been done. Solid-state lighting techniques are fundamentally made of luminescent materials [3]. In order to address the need greater use of low voltage lighting sources as a result of rising global energy consumption, RE doped solid-state substances are extremely fortunate and essential for energy-efficient and sustainable technology. These materials make use of the better higher emission efficiency, regulated emission profile, and sharp emission lines of other transition metal ion-doped inorganic materials. Due to their interesting optoelectronic, biochemical, and thermal properties [4]. Rare earth doped phosphors are the subject of present research because of their successful use in field emission displays (FEDs), luminescent paints, interior decoration, 3D display technology, tri-color lamps,

emergency lighting, safety indicators, white light-emitting devices, and agricultural fields [5].

The majority of luminescent substances (or phosphors) are solid inorganic substances made up of a host lattice that is typically purposefully doped. Energy is absorbed either through the host lattice or on impurities. Additionally, energy can be transferred through the lattice. Rare-earth ions, for example, which are only found in small proportions (a few moles percent or less), are the most common purposefully doped impurities on which the emission occurs. Numerous rare-earth-based host lattices or rare-earth ion-based luminous materials have been created in recent years. Many of these materials have been used in various applications. The performance of the devices in which rare-earth phosphors were used was frequently significantly improved [6].

One of the essential components of LED-based solid-state lighting technology is phosphor. It generates visible light by absorbing ultraviolet, violet, or blue light from LED chips. The performance of WLEDs, including luminous efficacy, colour rendering, correlated colour temperature, colour gamut, a long life, and so forth, is therefore greatly influenced by phosphor. Garnets, silicates, aluminates, phosphates, borates, and nitrides are only a few of the many substances that make good hosts for LED phosphors [7].

The rare earth calcium borate family, which also comprises additional compounds containing rare earth elements, includes CGBO. The alkaline earth lanthanide double borate group includes the $Ca_3Gd_3(BO_3)_4$ crystal. It is widely known that the $M_3Ln_2(BO_3)_4$ (M=Sr, Ca, Ln=Y, Gd) crystals are desirable choices as solid-state laser host materials [8]. As prospective phosphors for the white LEDs and plasma display panels, studies into the $M_3Ln_2(BO_3)_4$ compounds seeded with ions of rare earths have also been carried out [9]. Calcium Gadolinium Borate $Ca_3Gd_3(BO_3)_4$ is not available naturally as a mineral. It is a synthetic compound that is typically produced in the laboratory. However, it is structurally similar to naturally occurring borate minerals. Natural borate minerals that are similar in structure to CGBOO include datolite and vesuvianite. These minerals contain Boron, Calcium and other elements, but they do not specifically contain gadolinium.

The chemical formula of Calcium Gadolinium Borate is $Ca_3Gd_3(BO_3)_4$ and its molar mass is 967.31 g/mol. According to Fig.1 (a), the Calcium Gadolinium Borate unit cell is made up three sets of boron-oxygen BO_3 triangles and three sets of cation-oxygen polyhedral. Eight oxygen ions coordinate three distinct cation sites named M1, M2, and M3 (Figure 1b). Together with the M2O8 polyhedron, the M1O8 polyhedron shares oxygen atoms O6 and O7, while the M3O8 polyhedron shares atoms O3 and O7. In a three-dimensional framework, the Mj polyhedron connects the BO_3 triangles (Figure 1a). The M1, M2, and M3 sites are where the Ca^{2+} and Gd^{3+} ions are located, according to the distribution. The $Ca_3Gd_2(BO_3)_4$ lattice becomes physically disordered due to this sort of cation distribution, which results in the doped-RE ions' spectrum widening.
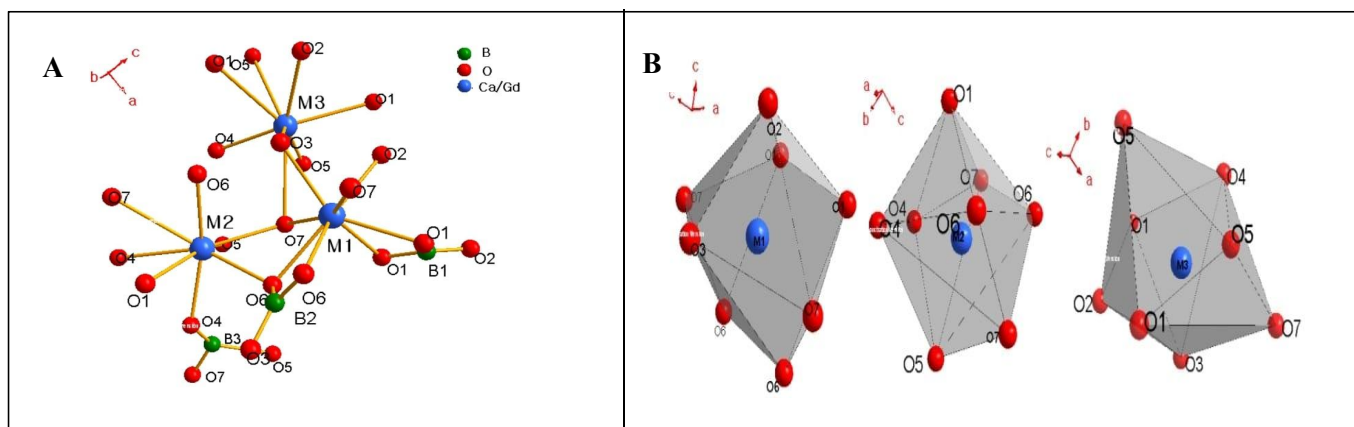

Figure 1. a) crystal Structure of CGBO b) and the coordination settings at the Ca^{2+} and Gd^{3+}ion's M1, M2, and M3 sites[10].

Pure CGBO is an odorless, fine pale-yellow powder. Its melting point is greater than 1000 °C and a density of 4.31 g/cm^3. It has the refractive index of typically 1.79 in the visible spectrum. exhibits good thermal stability at high temperatures [11]

CGBO consists of Calcium (Ca), Gadolinium (Gd), Boron (B) and Oxygen (O) atoms. CGBO is generally chemically stable and unreactive under normal conditions. It is insoluble in water and most common organic solvents. When heated to high temperatures, it decomposes to form boron oxide and the corresponding metal oxides.

$$3CaCO_3 + 2Gd_2O_3 + 4H_3BO_3 \rightarrow Ca_3Gd_2(BO_3)_4 + 6CO_2 + 2H_2O \ [11] \qquad Eq\text{-}(1)$$
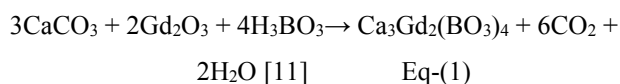
2. Materials and Methods

2.1 Overview of synthesis

Firstly, we collected the CGBO host material in the form of chemical substance using a weighing balance and then combining Calcium Carbonate ($CaCO_3$), Gadolinium Oxide (Gd_2O_3), and boric acid (H_3BO_3) as raw materials. These reactants were weighed and mixed in the stoichiometric ratio in the fashion to obtain a homogenous mixture as shown by the chemical equation (2).

$$3CaCO_3 + 2Gd_2O_3 + 4H_3BO_3 \rightarrow Ca_3Gd_2(BO_3)_4 + 6CO_2 + 2H_2O \qquad Eq\text{-}(2)$$
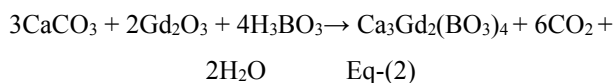
A number of clean plastic bottles were then filled with an equal volume of CGBO host material. In those bottles, the host material was mixed together with different molar quantities of dysprosium oxide (Dy_2O_3). Several alumina balls were placed in each of the bottles and the bottles were then sealed tightly with screw top plugs. To achieve good agglomeration of the powders, the bottles were ball milled for 1 hour. The ball milling process was performed, the powders were mixed well and placed in to small alumina crucibles with alumina lids and heated in the furnace at high temperature before the onset of the melting point for approximately 10 hours. The sintering process was carried out by the heat and cooling rate as low as 100 ^{0}C/ hr. The sintered powders were synthesized from alumina crucibles. The obtained product is once more grounded to acquire small particles and then siftings are carried out to get rid of large survivals.

The solid-state reaction method is quite inexpensive and uncomplicated for synthesizing dysprosium doped calcium gadolinium borate material. However, it may result in inhomogeneous and whiter infested powders due to incomplete reaction or contaminated furnace atmosphere. As heating conditions play massive roles in determining the quality of the phosphorescent material, high purity of the starting materials is crucial.

2.2 Solid-State reaction method preparation

$Ca_3Gd_2(BO_3)_4:Dy^{3+}$ phosphors were synthesized employing the conventional solid state reaction method. Another frequently used approach for making dysprosium-doped calcium gadolinium borate. The method that can create Dy^{3+} phosphorescent material is through the solid-state reaction method. With the use of this method of producing the end product, the individual components are mixed in the right proportion in terms of stoichiometry and then exposed to high temperature in a furnace.

The solid-state reaction method is less time consuming and cost effective for synthesizing dysprosium doped calcium gadolinium borate material. It could nevertheless create inhomogeneity and impurities in the finished product, because of unsaturated reactions or the influence of the furnace atmosphere, however. Achieving a high quality phosphorescent material is ensured by strict regulation of the heating process as well as the usage of highly pure initial components.

2.3 Material required

The host and doping material should be employed in their purest forms to produce $Ca_3Gd_2(BO_3)_4$ phosphor in order to achieve superior results [12].

2.4 Quantity

For the best results, the correct host and dopant materials should be used in the solid-state reaction process. The

82

luminous properties of the phosphor are influenced by the host to doping agent ratio.

2.5 Characterization

At the Centralized Resource Laboratories, Department of the Physics University of Peshawar, XRD, SEM, and analyses have been used to examine the uniform morphology, phase purity, and crystallinity of the synthesized samples. The samples will be subjected to optical analysis utilizing the UV-Vis spectroscopy equipment at the MRL, Department of the Physics University of Peshawar.

3. Results and discussion

3.1 X-ray diffraction analysis (XRD)

Figure 2 compares the XRD peaks of $Ca_3Gd_2(BO_3)_4:Dy^{3+}$ rare earth doped phosphors with reference peaks of $Ca_3Gd_2(BO_3)_4$ (PDF No. 48-0293). The required phase is achieved for the synthesized phosphors because the peaks of our compound match well with the peaks of the reference compound. This also further verifies that the synthetic phosphors have tetrahedral structures with the similar numbers of atoms. Further, we can use Bragg's diffraction formula to measure the various lattice parameters of the synthesized phosphors which will in turn help to explain the structure of the compound. Additionally in Figure 2, the XRD patterns of $Ca_3Gd_2(BO_3)_4:Dy^{3+}$ are compared with the XRD peaks of accepted PDF references of Joint Committee on Powder Diffraction Standards (JCPDS) PDF No. 48-0293. The following comparison highlights the fact that none of the synthesized phosphors contain any extra peaks of the constituent components. Therefore, it was found that the reactants used in the preparation procedure did not cause any contamination to the synthesized materials which were all, single phase.

3.2. SEM micro structural analysis

For the better understanding of the SEM images of the synthesized products at various dopant concentrations, figures 3 (a) and (b) are provided separately. These micrographs show how the nature of the particles differs depending on their morphologies and forms. To attain high brightness, the phosphor must be crystalline and the size of the grains in the phosphor must be less than one micron.
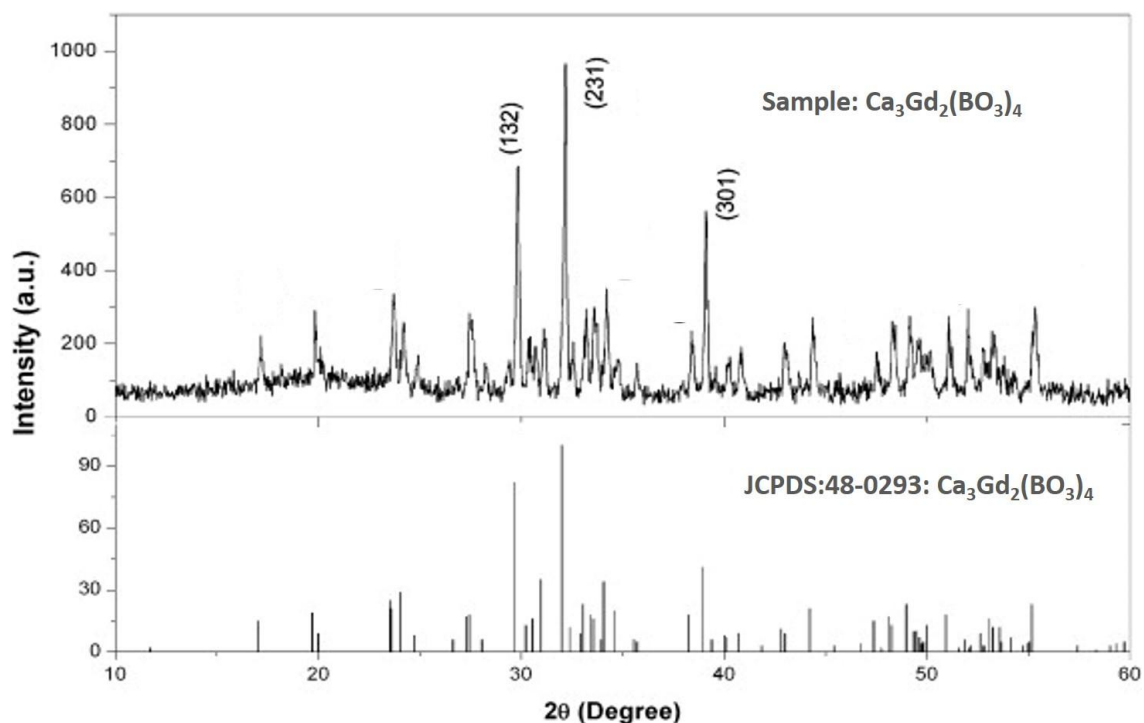

Figure 2. XRD peaks of $Ca_3Gd_2(BO_3)_4:Dy^{3+}$ doped with rare earth elements.

The synthesized phosphors will have good luminescence since the sizes of phosphor grains are in the micrometer scale. It is difficult to predict what novel phosphors with micrometer-sized grains may prove useful in future X-ray imaging applications using sing Scherrer's equation [13]. a rough estimation of the mean grain size "D" of the crystallite could be made.

$$D = \frac{k\lambda}{\beta(2\theta)\cos\theta} \quad [13] \quad Eq\text{-}(3)$$

The symbols used in the β (2θ) equation include radian measurement of the pure diffraction profile; the constant value of k; the X-ray wavelength; diffraction angle; and "D" stands for average grain size. As it can be seen from the phosphor's XRD patterns represented by the primary peaks in Figs. 3a and 3b, the grain size can be calculated using Scherer's equation that determines the size of crystallites.
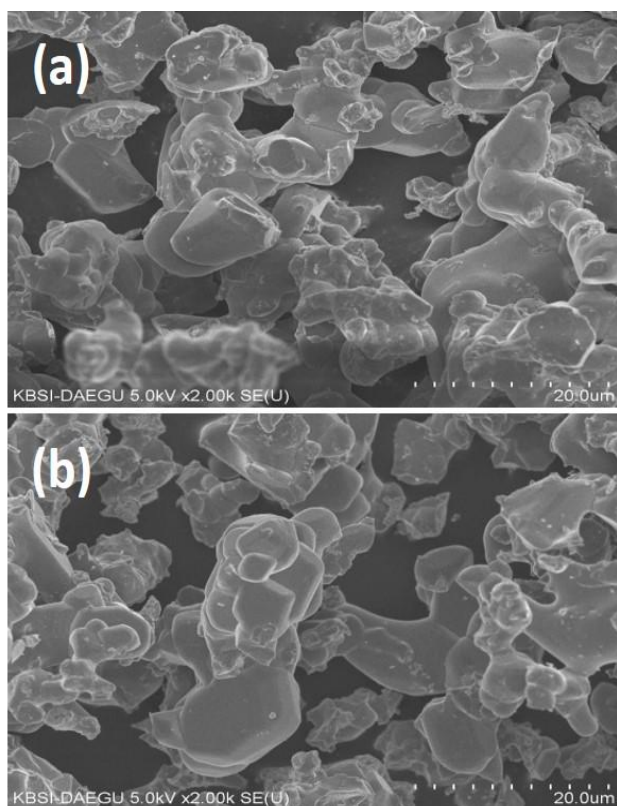

Figure 3. SEM Micrographs of (a) Pure $Ca_3Gd_2(BO_3)_4$ (b) $Ca_3Gd_2(BO_3)_4:Dy^{3+}$ (2 mol%)

Pure CGBO sample and Dy doped ($Ca_3Gd_2(BO_3)_4:Dy^{3+}$) of 2 mole% the SEM images are presented in the figure 3 (a) and (b) The grain size is almost similar of the pure $Ca_3Gd_2(BO_3)_4$

phosphor sample and 2 mole% of Dy doped sample. Therefore, it could be deduced that the grain size of the samples does not influence the luminescence.
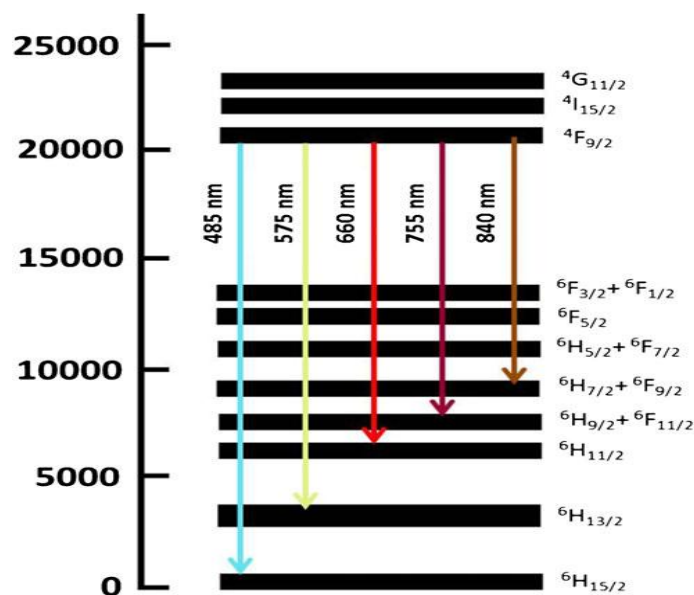

Figure 4. Energy level diagram for Dy^{3+}

3.3 UV luminescence of $Ca_3Gd_2(BO_3)_4:Dy^{3+}$

The energy level diagram for the Dy^{3+} ion transitions in the $Ca_3Gd_2(BO_3)_4$ phosphor is shown in Figure 4. It displays the levels of the host and Dy^{3+} dopant's valence and conduction bands. The host $Ca_3Gd_2(BO_3)_4$ valence and conduction bands sandwich the dopant Dy^{3+} valence and conduction bands. While other excitations may be conceivable in this range, $^6H_{15/2}$ - $^4M_{15/2}$+ $^6M_{7/2}$ is the band where they are most likely to occur.

Additionally, it displays the emission bands of the Dy^{3+} doped synthetic material. $^4F_{9/2}$ - $^6H_{9/2}$ + $^6F_{11/2}$, $^4F_{9/2}$ - $^6H_{11/2}$ + $^6F_{13/2}$, $^4F_{9/2}$ -$^6H_{15/2}$, and $^4F_{9/2}$ -$^6H_{11/2}$ are the emission transitions. While $^4F_{9/2}$-$^6H_{13/2}$ (yellow) and $^4F_{9/2}$ -$^6H_{15/2}$ (blue) are the more dominating peaks, blue/yellow color applications place a greater emphasis on the former. However, it was applicable in red due to the presence of $^4F_{9/2}$ -$^6H_{11/2}$ (red) emission transitions. The usage of this phosphor as a multicolor phosphor is also possible.

Figure 5 depicts the emission spectra of $Ca_3Gd_2(BO_3)_4:Dy^{3+}$, which were also detected. The ground state is the source of

84

all excitations. Two significant emission peaks are depicted in Figure 5 peak 483 nm having transition $^4F_{9/2}$-$^6H_{15/2}$ and peak 576 nm having transition $^4F_{9/2}$-$^6H_{13/2}$. Between the range of 650nm and 790nm, additional minor emission peaks are seen. This can be employed in multi-color applications due to its multi-color emissions peaks.

The presence of distinctive emissions attributed to Dy^{3+} offers confirmation of the luminescent behavior of Dy^{3+} ions within the $Ca_3Gd_2(BO_3)_4$ host. Comparable distinct emissions have been noted in Dy^{3+} doped aluminates such as $SrAl_2O_4$ [14],$CaAl_2O_4$ [15] , $MgAl_2O_4$ [16] , as well as in a series of silicates [17-23].
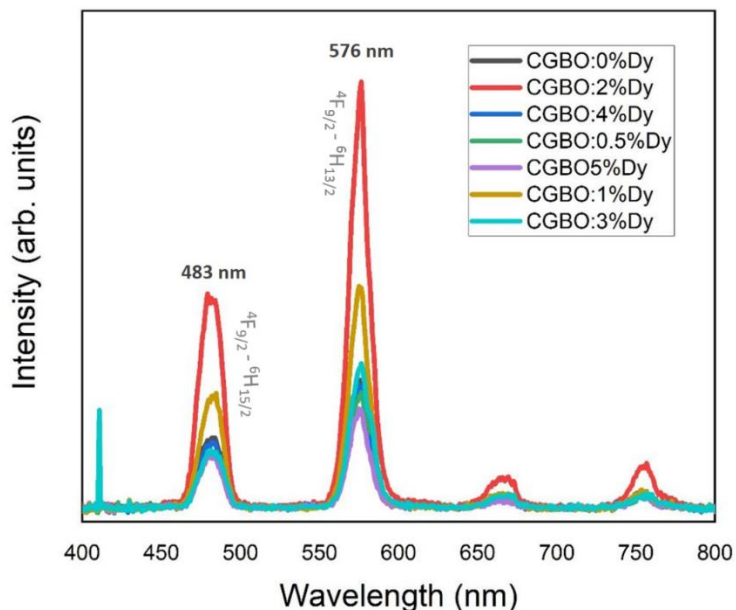

Figure 5. Emission spectra of $Ca_3Gd_2(BO_3)_4$:Dy^{3+} phosphor by UV light.
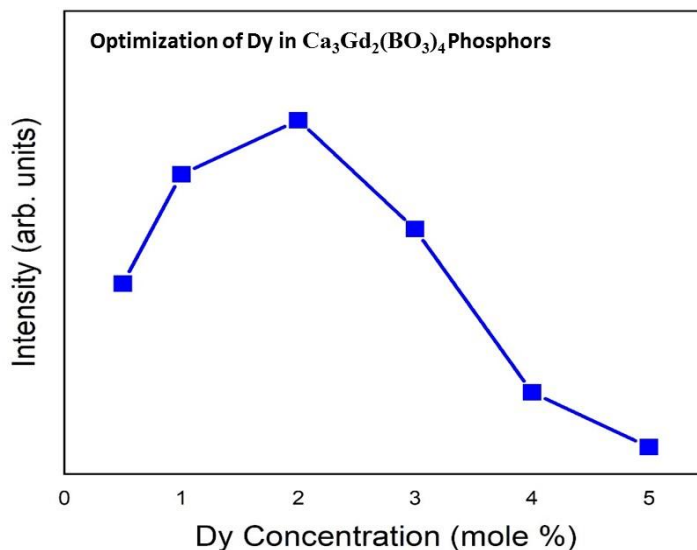

Figure 6. Optimization of Dy in $Ca_3Gd_2(BO_3)_4$ phosphor.

4. Conclusion

In this study, we successfully synthesized Dysprosium doped

Calcium Gadolinium Borate ($Ca_3Gd_2(BO_3)_4$. Intensely green-emitting Dy^{3+} activated phosphors have been synthesized through a conventional solid-state synthesis method. The

substrate samples for the study were prepared in such a way that they contain different concentrations of Dy^{3+} ion, namely 0.5 mole%, 1mole%, 2mole%, 3mole%, 4mole% and 5mole% respectively, after which structural and luminescent properties were investigated. X-ray diffraction (XRD) analysis confirmed the formation of a pure phase of $Ca_3Gd_2(BO_3)_4$. As for the Dy^{3+} ions, a good relocation independent on dopant concentration was observed after 10h of heating at 800°C. The presence of Dy^{3+} ions in the host lattice can thus be affirmed without the introduction of other undesirable phases.

The result of photoluminescence (PL) analysis indicated that the intensity of the emission was also highest at 2 mole% Dy^{3+} concentration. Emission spectra have displays the characteristic peaks of 483nm and 576nm corresponding to the blue and yellow regions respectively are due to the transition of $^4F_{9/2} \rightarrow {}^6H_{15/2}$ and $^4F_{9/2} \rightarrow {}^6H_{13/2}$ respectively. These observations call for future work on Dy^{3+} doped $Ca_3Gd_2(BO_3)_4$ phosphors because they could be used as tunable yellow phosphors in optoelectronic devices.

At the same time, the synthesized materials possessed characteristics similar to medical diagnostic imaging facilities, including the X-ray and CT scans. This creates other opportunities for these materials in the medical and diagnostic imaging where luminescent materials are used to identify internal structures. The emission characteristics of Dy^{3+} doped $Ca_3Gd_2(BO_3)_4$ phosphors, tunable color and its potential as the biomedical imaging tool make it an excellent candidate for various technological applications; solid state lighting, display devices and biomedical diagnostic tools.

In conclusion, the successful synthesis and comprehensive analysis of Dy^{3+} doped $Ca_3Gd_2(BO_3)_4$ phosphors are illustrated with their potential in legitimate optoelectronic and medical imaging applications.

Authors Contribution

Majid Ali and Hammad Haider are co-first authors, both contributing equally to all experimental work. Additionally, Majid Ali and Hammad Haider took responsibility for writing the manuscript. Associate Professor Dr. Fawad Ullah and Muhammad Bilal acted as the corresponding authors. Additionally, Dr. Fawad Ullah guided the work, supervised the research, and revised the manuscript. Shahzad Nawaz Malik contributed to analysis of XRD results.

Conflicts of Interest

The author declares no known competing financial interests or personal relationships that could have appeared to influence the work reported in this paper

Data Availability statement

The data presented in this study are available on request from the corresponding author.

REFERENCES

1. Bilal, M., Ali, M., Haider, H., Anwar, S., Ahmad, S., & Jamshed, M., 2024. Green Synthesis and Photoluminescence Study of Dy-Doped CaCO3. Journal of Chemistry and Environment, pp. 58-67.

2. Xia, S., Wang, T., Ren, Z., Yang, X., Guo, Q., & Zhou, C., 2024. Adsorption Structure–Activity Correlation in the Photocatalytic Chemistry of Methanol and Water on TiO2 (110). Accounts of Chemical Research, pp. 2620-2630.

3. Ardiçoğlu, B., Özbayoğlu, G., Özdemir, Z., and Yilmaz, A., 2006. Production and identification of rare-earth doped lithium triborate. Journal of Alloys and Compounds, 418, pp. 77-79.

4. Arulraj, A., Santhosh, P., Gopalan, R. S., Guha, A., Raychaudhuri, A., Kumar, N., et al., 1998. Charge ordering in the rare-earth manganates: The origin of the extraordinary sensitivity to the average radius of the A-site cations. Journal of Physics: Condensed Matter, 10, p. 8497.

5. Premkumar, A., Weiland, C., Hwang, S., Jäck, B., Place, A. P., Waluyo, I., ... & Jarrige, I., 2021. Microscopic relaxation channels in materials for superconducting qubits. Communications Materials, 2(1), p. 72.

6. Ryu, S., Kim, K., Kim, J. Y., Cho, I. K., Kim, H., Ahn, J., ... & Ahn, S., 2022. Design and analysis of a

86

magnetic field communication system using a giant magneto-impedance sensor. IEEE Access, 10, pp. 56961-56973.

7. Beatty, A. E., Esco, A., Curtiss, A., and Ballen, C., 2022. Students who prefer face-to-face tests outperform their online peers in organic chemistry. Chemistry Education Research and Practice.

8. Kądzielawa, A., 2021. First-principle approach to electronic states and metal-insulator transition in selected correlated model systems. Doctoral dissertation.

9. Abboushi, B., Fotios, S., & Miller, N. J., 2024. Predicting discomfort from glare with pedestrian-scale lighting: A comparison of candidate models using four independent datasets. Lighting Research & Technology, 56(3), pp. 225-246.

10. Chahara, K. i., Ohno, T., Kasai, M., and Kozono, Y., 1993. Magnetoresistance in magnetic manganese oxide with intrinsic antiferromagnetic spin structure. Applied Physics Letters, 63, pp. 1990-1992.

11. Chen, J., Li, Y., Song, G., Yao, D., Yuan, L., and Wang, S., 2006. Growth and characterization of pure $Li_6Gd(BO_3)_3$ single crystals by the modified Bridgman method. Journal of Crystal Growth, 294, pp. 411-416.

12. Magyari-Köpe, B., Tendulkar, M., Park, S.-G., Lee, H. D., and Nishi, Y., 2011. Resistive switching mechanisms in random access memory devices incorporating transition metal oxides: TiO_2, NiO, and $Pr_{0.7}Ca_{0.3}MnO_3$. Nanotechnology, 22, p. 254029.

13. Maleki Dizaj, S., Barzegar-Jalali, M., Zarrintan, M. H., Adibkia, K., and Lotfipour, F., 2015. Calcium carbonate nanoparticles as cancer drug delivery systems. Expert Opinion on Drug Delivery, 12, pp. 1649-1660.

14. Moore, T. P., 2010. Ilfeld Harz Mountains: Thuringia, Germany. The Mineralogical Record, 41, pp. 481-506.

15. Moshnyaga, V., Khoroshun, I., Sidorenko, A., Petrenko, P., Weidinger, A., Zeitler, M., et al., 1999. Preparation of rare-earth manganite-oxide thin films by metalorganic aerosol deposition technique. Applied Physics Letters, 74, pp. 2842-2844.

16. Huang, Y. M., and Ma, Q.-l., 2015. Long afterglow of trivalent dysprosium-doped strontium aluminate. Journal of Luminescence, 160, pp. 271-275.

17. Liu, B., Shi, C., and Qi, Z., 2005. Potential white-light long-lasting phosphor: Dy3+-doped aluminate. Applied Physics Letters, 86, p. 021909.

18. Omkaram, I., and Buddhudu, S., 2009. Photoluminescence properties of $MgAl_2O_4$: Dy3+ powder phosphor. Optical Materials, 32, pp. 8-11.

19. You, P., Yin, G., Chen, X., Yue, B., Huang, Z., Liao, X., et al., 2011. Luminescence properties of Dy3+-doped Li_2SrSiO_4 for NUV-excited white LEDs. Optical Materials, 33, pp. 1808-1812.

20. Liu, B., Kong, L., and Shi, C., 2007. White-light long-lasting phosphor $Sr_2MgSi_2O_7$: Dy3+. Journal of Luminescence, 122, pp. 121-124.

21. Chen, Y., Cheng, X., Liu, M., Qi, Z., and Shi, C., 2009. Comparison study of the luminescent properties of the white-light long afterglow phosphors: $Ca_xMgSi_2O_{5+x}$: Dy3+ (x = 1, 2, 3). Journal of Luminescence, 129, pp. 531-535.

22. Kuang, J., Liu, Y., and Zhang, J., 2006. White-light-emitting long-lasting phosphorescence in Dy3+-doped $SrSiO_3$. Journal of Solid State Chemistry, 179, pp. 266-269.

23. Liu, Y., Lei, B., and Shi, C., 2005. Luminescent properties of a white afterglow phosphor $CdSiO_3$: Dy3+. Chemistry of Materials, 17, pp. 2108-2113.